Ammonium alum hydrate slurries with surfactants and polyvinyl alcohol as a latent heat transportation material for high temperature

Hidema, Ruri
Tano, Takuya
Sato, Hideki
Komoda, Yoshiyuki
Suzuki, Hiroshi

(Citation)
International Journal of Heat and Mass Transfer,124:1334-1346

(Issue Date)
2018-09

(Resource Type)
journal article

(Version)
Accepted Manuscript

(URL)
https://hdl.handle.net/20.500.14094/90005051

Ammonium alum hydrate slurries with surfactants and polyvinyl alcohol as a latent heat transportation material for high temperature

Ruri Hidema*, Takuya Tano, Hideki Sato, Yoshiyuki Komoda, Hiroshi Suzuki

Department of Chemical Science and Engineering, Kobe University, Kobe 657-8501, Japan

*Corresponding Author
Phone: +81-78-803-6657
Fax: +81-78-803-6657
hidema@port.kobe-u.ac.jp

Ammonium alum hydrate is a promising material for a latent heat transportation system for higher temperature around 50°C. However, there were two big problems to be solved. One is a low fluidity of the slurries due to increasing the viscosity; the other is a sedimentation of phase changed ammonium alum hydrate particles in the slurry due to high density of the particle, which causes pipe blockage. In this study, in order to solve these problems, we added drag reducing surfactants and polyvinyl alcohol (PVA) to the ammonium alum hydrate solution, and investigated the effects of them. Particle growth and sedimentation of ammonium alum in the solution were prohibited by adding both surfactants and PVA. Addition of only PVA to ammonium alum solution didn't prevent the particle growth and the sedimentation. That is, the effect was a synergetic effect. In order to understand the synergetic effect, inner structures of a solution containing surfactants and PVA were measured by a dynamic light scattering (DLS). Flow and heat transfer characteristics were also measured and analyzed. Friction coefficients of solutions and slurries were decreased with the drag reducing surfactants, which was not affected by addition of PVA. Heat transfer characteristics of ammonium alum hydrate slurries were higher than that of solution with surfactants and PVA. All the results confirmed the applicability of the ammonium alum hydrate slurries for the high temperature latent heat transportation systems.

Keywords: Latent Heat Transportation, Hydrate Slurry, Two-phase/Multiphase flow, Particle Sedimentation, Drag-reducing Agents

1. Introduction

For utilization of waste heat, it is required to solve a problem called thermal gap problem that is a time and space gaps between a utilization area and a supplier [1]. It is important to transfer the waste heat to the utilization area without much temperature variation. Here, latent heat transportation is a promising technique to

transfer the waste heat efficiently. For example, phase change slurries containing fine particles with large latent heat have great advantages as secondary refrigerants [1]. This is because the slurry sustains temperature during the transportation due to a large apparent heat capacity. Therefore, the latent heat transportation increases the efficiency of the transportation.

A phase change material used for a latent heat transportation system is selected based on a temperature demanded in a system. Different types of latent heat slurries have been used in industries [1-5]. Ice/water slurries are one of the most common secondary refrigerants for low temperature [5-9]. One of an example to use ice/water slurries is a food cold chain to keep foods fresh. The ice/water slurry is also used in a tube as heat transfer media of cooling circular systems. In that case, there was a famous problem: The agglomeration of ice particles in slurries, which induces a problem of a pipe blockage. In order to solve the problem, a number of studies about ice slurries have been made. Several techniques to prevent the agglomeration of ice particles was proposed by many researches [4]. Anti-freeze protein (AFP), silane coupling agents and polyvinyl alcohol (PVA) are known to prevent the agglomeration and the particle growth [10-15]. Some kinds of brines and surfactants were also believed as anti-agglomeration agents [7]. However, the effects of brines and surfactants to prevent the agglomeration of ice particles in slurries are limited based on its concentration [15]. In addition, the surfactants prevented the crystal growth and the agglomeration more effectively with PVA additives [16, 17].

For slightly higher temperature, clathrate hydrate slurries such as tetrabutylammonium bromide (TBAB) and trimethylolethane hydrates are well known. Flow characteristics and heat transfer characteristics of TBAB and trimethylolethane hydrates have been reported in many previous studies [2, 17-23]. Since trimethylolethane slurry shows highly viscous non-Newtonian flow behaviors, some researchers added drag-reducing surfactants that form rod-like micelles to improve the fluidity [20, 24-29].

While many studies have been performed for low temperature latent heat slurries, a few studies have been made for higher temperature over 30 °C. Suzuki et al. [30] discussed the applicability of inorganic disodium hydrogen phosphate dodecahydrate slurries for a cooling system of absorption chillers: The inorganic hydrate slurry has a phase change temperature of 35 °C.

For further higher temperature, aluminum ammonium sulfate disodium dodecahydrate (ammonium alum hydrate) is only the material that firstly proposed in our previous studies [16, 31, 32]. Ammonium alum hydrate is an inorganic material whose latent heat is 251 $kJ \cdot kg^{-1}$. The phase change temperature of ammonium alum hydrate is controlled by its concentration in solution. The phase change temperature is 51°C at the concentration of 35 wt%. 51°C is a suitable temperature for district heating system or for domestic use of hot water. Indeed, the thermal energy consumption for air-conditioning and hot water supply in residential and commercial areas in Japan is 50 to 60% of total energy consumption of these areas [1, 33]. Therefore, to establish a system to transport the waste heat from industry around 50°C can save much energy. Thus, ammonium alum hydrate seems a very promising slurry.

However, there are two big problems required to be solved. One is low fluidity of the slurry and the other is sedimentation of ammonium alum hydrate particles in fluids. The low fluidity is due to high viscosity of the slurry. Therefore, we proposed to add drag-reducing cationic surfactants to ammonium alum hydrate slurries to reduce the friction coefficient [31]. The sedimentation problem is due to the high density of 1630 $kg \cdot m^{-3}$. The sedimentation of phase changed particles attached to the wall reduces heat transfer efficiency and induces pipe blockage. In the case of a latent heat medium for lower temperature such as ice slurries, pipe blockage is easily solved when the system stops at room temperature. This is because the latent heat medium is melted at room temperature. On the other hand, in the case of a latent heat medium for higher temperature, once sedimentation and pipe blockage occur, the situation will be even worse when the system stops. This is because the phase change temperature of the latent heat medium is higher than room temperature. Therefore, to prevent the sedimentation is highly demanded. In our previous study, we have tested the effects of polyvinyl alcohol (PVA) as a stabilizer for preventing the sedimentation [32]. PVA was selected since it had been reported that PVA prevents ice growth [16, 17] and did not disturb drag-reducing effects of zwitter-ion surfactants in the slurry [16]. Indeed, PVA and drag-reducing surfactants showed a synergistic effect. The sedimentation and the crystal growth of ammonium alum hydrates were effectively prohibited only when both PVA and surfactants were added to the slurry [32]. However, the interaction between surfactants and PVA has not been investigated yet.

In this study, effects of surfactants and PVA mixture on sedimentation and particle growth of ammonium alum hydrate were precisely analyzed. In addition, a single effect of PVA on sedimentation and particle growth were also observed. In order to investigate the interaction between surfactants and PVA, inner structures of surfactants and PVA solution were measured by dynamic light scattering. Fluidity and heat transfer characteristics of ammonium alum hydrate solution and slurry were also measured. Sedimentation of the particles in fluids of the slurries was visualized by a tomography method.

2. Experimental Procedures

2.1. Materials

Each solution contains aluminum ammonium sulfate disodium dodecahydrate (ammonium alum hydrate: $AlNH_4(SO_4)_2 \cdot 12H_2O$, Wako pure chemical) as an inorganic latent heat material at the concentration of 35 wt%. The latent heat of the hydrate is 251 $kJ \cdot kg^{-1}$. As reported in our previous studies [31], its phase change temperature is 51°C when its concentration in water is 35 wt%.

A cationic surfactant, behenyl trimethyl ammonium chloride (Arquad 22/80, Lion Specialty Chemicals CO.,LTD.), was used as drag-reducing additives. Sodium salicylate was used as the source of counter-ions required for forming rod-like micelles of the surfactants. The surfactants exhibit effective drag reduction in water in the temperature range from 40°C to 80°C: This is because the rod-like micelles of the surfactants is formed at the temperature range. In this study, when a solution contains the surfactants, the concentration of the surfactant was kept at 2,000 ppm; the molar ratio of the counter-ions to the surfactants was fixed at 1.5.

Polyvinyl alcohol (PVA, Wako pure chemical) of full saponification and of 500 polymerization was selected as a stabilizer preventing particle sedimentation. The concentrations of PVA were changed from 0 to 14,000 ppm.

The precise concentration of each sample solution for viscosity measurements, sedimentation observations, growth of the particle size observations, is shown Table 1 and 2.

Table 1. Concentration of each material in each solution

Sample name	1	2	3	4	5	6	7	8	9
Ammonium alum hydrate, [wt%]	35	35	35	35	35	35	35	35	35
Surfactant, [ppm]	0	2000	2000	2000	2000	2000	2000	2000	2000
Polyvinyl alcohol, [ppm]	0	0	100	200	300	400	500	1000	2000

Table 2. Concentration of each material in each solution

Sample name	10	11	12	13	14	15	16	17	18
Ammonium alum hydrate, [wt%]	35	35	35	35	35	35	35	35	35
Surfactant, [ppm]	0	0	0	0	0	0	0	0	0
Polyvinyl alcohol, [ppm]	100	200	500	1000	2000	4000	7000	10000	14000

2.2. Viscosity measurements

Viscosities of ammonium alum hydrate solutions and slurries with and without the surfactants and PVA were measured by a rheometer (Anton Paar, MCR301). A parallel-plates device having a diameter of 50 mm and a gap of 1 mm was used for the measurements. The viscosity measurements of the ammonium alum hydrate slurry were performed at 50 °C: The hydrate fraction was 12 wt%. The viscosity measurements of the ammonium alum solution were performed at 60°C. The shear rate was ranged from 10 to 1000 s^{-1} during the viscosity measurements. Since fluids containing rod-like micelles show shear thinning, the formation of rod-like micelles in each sample was confirmed by the viscosity measurements.

2.3. Sedimentation observations of the ammonium alum hydrate particles

The effects of PVA on sedimentation phenomena of ammonium alum hydrates were observed. Ammonium alum hydrate was completely dissolved at a higher temperature. The solution was cooled until 50°C with stirring as hydrates appeared smoothly, and then 25 ml of the solution was poured into test tubes. The test tubes were set in a water bath: The temperature was kept constant at 50°C (Fig.1(a)). The test tubes were shot by a digital camera. In the case of both surfactants and PVA added solution, the sedimentation was observed for 5 days. In the case of only PVA added solution, the sedimentation was observed for 3 days, since ammonium alum hydrate was totally settled out in the 3 days. The

sedimentation was quantified by an apparent dispersion fraction: A sedimentation length was divided by an initial length (Fig.1(b)).

2.4. Growth process observations of the ammonium alum hydrate particles

The growth of particles of ammonium alum hydrate was observed under a microscope in order to observe how surfactants and PVA affect crystallizations of ammonium alum hydrate (Fig.1(c)). The ammonium alum hydrate was completely dissolved at a higher temperature. The solution was stirred at 50°C to obtain small particles. The small particles with small amount of solutions were placed to a Petri dish: The temperature was kept constant at 50°C. The depth of solutions in the Petri dish was less than 3 mm. The Petri dish was set under a microscope. A focal length of an objective lens was 34 mm. The hydrate particles in the Petri dish were shot by a camera attached to the microscope. In order to measure the particle sizes, more than 300 particles were selected by an image processing software. Each particle was fit by each equivalent circle: The diameter of the circle was measured as the diameter of the particles. The growth process of the particle was observed until 6 hours after particle generation.

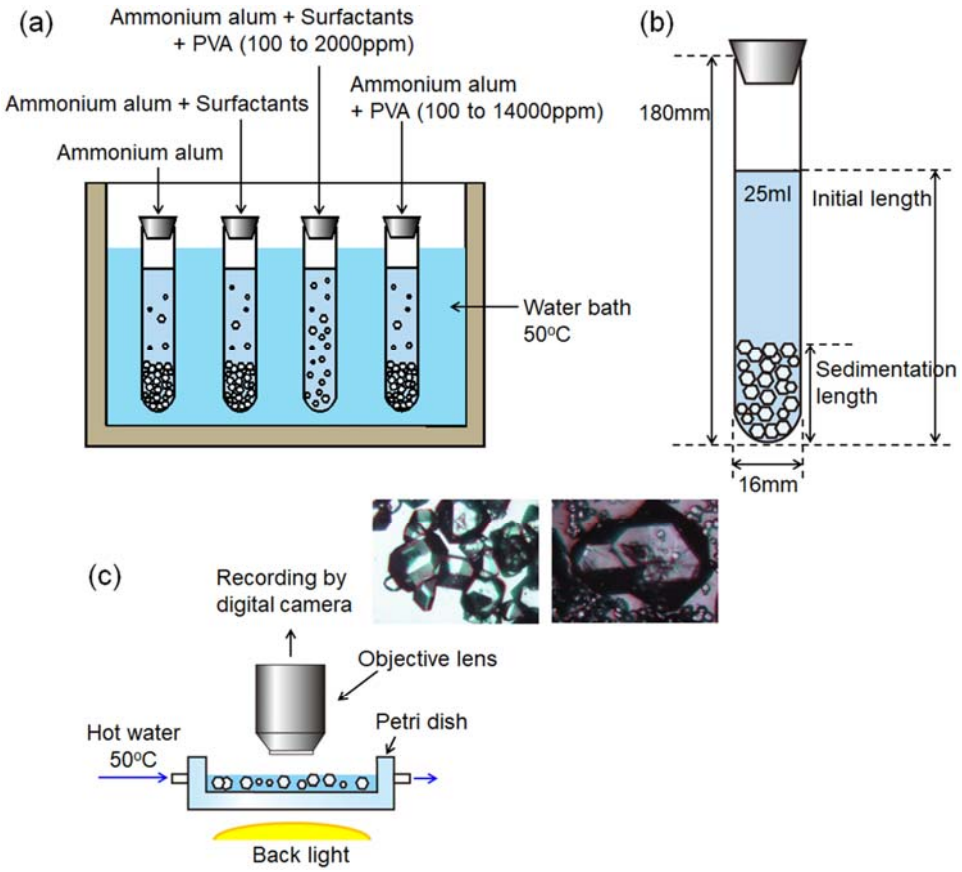

Fig.1 Schematic of the experimental apparatus to observe sedimentation phenomena and growths of the particle sizes.

2.5. Dynamic light scattering experiments

It is important to identify the effects of surfactants and PVA on the sedimentation and the crystallization of ammonium alum hydrate. Thus, a dynamic light scattering system (DLS, Photal Otuka Electronics, DLS-7000) was used to measure inner structures of surfactants and PVA solutions. 1000 ppm PVA solution, 2000 ppm surfactant solution with counter ions, and the mixture of the surfactants and PVA were measured. The precise concentration is shown in Table 3. Wavelength of the laser beam was 632.8 nm. Temperature of the sample was set at 50°C.

In this experiment, ammonium alum hydrate was not dissolved in the solutions. Since ammonium alum hydrate crystalizes in sample solution, the crystals can disturb DLS measurements. Besides, ammonium alum hydrate does not affect formations of rod-like micelles, which was confirmed by viscosity measurements (Fig. 4). Therefore, it is reasonable to measure sample solutions containing only surfactants and PVA without ammonium alum hydrate.

Table 3. Concentration of each material in each solution for DLS experiments

Sample name	A	B	C	D	E	F
Ammonium alum hydrate, [wt%]	0	0	0	0	0	0
Surfactant, [ppm]	0	2000	2000	2000	2000	2000
Polyvinyl alcohol, [ppm]	1000	0	200	500	1000	2000

2.6. Friction coefficient and heat transfer coefficient measurements

Figure 2 shows an experimental apparatus for measuring friction and heat transfer coefficients of hydrate solutions and slurries. The solution of ammonia alum hydrate was prepared in a heating tank heated by a handy-heater: The solution was supplied to the test section through the entry section with a length of 2.5 m by using a pump. The test section was made of a stainless steel tube with a length of 2 m, an inner diameter, D_i [m], of 13 mm and an outer diameter, D_o [m], of 18 mm. The cross section area of the test section is shown in Fig.2 and Fig.3(a). The temperature at the test section was controlled by an outer tube with the inner diameter, D_x [m], of 25 mm.

During the measurement of friction coefficients, the outer flow temperature was maintained equal to the inner flow temperature for preventing any phase change of hydrates. The inlet temperature was set at 60°C for pressure difference measurements for solutions. At 60°C, no hydrate particles exist. The inlet temperature was kept constant at 50°C for pressure difference measurements for slurries. Hydrate mass fraction of the slurry, H_f [wt%], was 12 wt%. Pressure difference between the inlet and outlet of the inner tube was measured using a pressure difference transducer.

We have measured heat transfer coefficient of solution and slurry of each sample, and water to validate the experiments. For a measurement of heat transfer coefficients on solutions, fluid temperature in the inner tube was maintained higher than 60°C. To measure the heat transfer coefficients on slurries, fluid temperature in the inner tube was decreased from about 54 °C to 51 °C in the test section. At the temperature rage, solidification of hydrates occurs in the test section, and the hydrate mass fraction was 12 wt% at the outlet. The test section was cooled by passing cold water through the outer tube. The inlet and outlet temperatures of the slurry flowing though the inner tube were measured by thermocouples; the inlet and

outlet temperatures of cold water flowing to the opposite direction through the outer tube were also measured. The inner flow mean velocity, U_m [m・s^{-1}] ranged from 0.7 to 5.2 m/s. As described later, supercooling did not occur during the solidification process: Pump pressure helped to prohibit supercooling. In addition, we have confirmed the solidification process at the phase change temperature by using the tomography method.

The following Dittus-Boelter's equation was assumed to estimate heat transfer from the wall of the inner tube to water in the outer tube.

$$Nu_w = 0.023 Re_w^{0.8} Pr_w^{0.4} \quad (1)$$

Here, Nu_w[-] is , Re_w [-] and Pr_w [-] are Nusselt number, Reynolds number and Prandtl number respectively based on water properties.

$$Nu_w = \frac{\alpha_w D_h}{\lambda_w} \quad (2)$$

$$Re_w = \frac{\rho_w U_o D_h}{\eta_w} \quad (3)$$

$$Pr_w = \frac{c_w \eta_w}{\lambda_w} \quad (4)$$

Here, α_w [W・m^{-2}・K^{-1}] is the heat transfer coefficient from the inner tube to the fluid through the outer tube; U_o [m・s^{-1}] is cross-sectional mean velocity flowing between the inner and the outer tubes; D_h [m] is the hydraulic diameter of the flow path between the inner tube and the outer tube (= D_x - D_o). λ_w [W・m^{-2}・K^{-1}] is water thermal conductivity; ρ_w [kg・m^{-3}] is water density; η_w [Pa・s] is water viscosity; c_w [J・kg^{-1}・K^{-1}] is water specific heat capacity.

With Eq. (1), the outer heat transfer coefficient, α_o [W・m^{-1}・K^{-1}], was calculated. The overall heat transfer coefficient, K [W・m^{-1}・K^{-1}] was measured by the logarithmic mean temperature by the thermocouples inserted into the inlets and outlets both in the outer and inner tubes. The inner heat transfer coefficient, α_i [W・m^{-1}・K^{-1}], was calculated by the following equation.

$$\frac{1}{K}=\left[\frac{1}{\alpha_{\mathrm{i}}}+\frac{1}{\alpha_{\mathrm{o}}}\frac{D_{\mathrm{i}}}{D_{\mathrm{o}}}+\frac{\delta}{\lambda_{\mathrm{c}}}\frac{D_{\mathrm{i}}}{D_{\mathrm{i}}-D_{\mathrm{o}}}\ln\left(\frac{D_{\mathrm{i}}}{D_{\mathrm{o}}}\right)\right] \tag{5}$$

Here, λ_c [W・m^{-2}・K^{-1}] and δ [m] are the thermal conductivity of the tube made of copper and the thickness of the tube. In the cases including the phase change materials, the inner heat transfer coefficients are over estimated with this kind of calculations, which includes the contribution of phase changes. In the present study, the difference between water and phage change material slurries will be discussed. Then, this apparent heat transfer coefficient including the phase change effect was adopted.

In order to discuss the effect of additives, the non-dimensional parameters based on the ammonium alum hydrate solution properties without any additives, Nu_s [-], Re_s [-] and Pr_s [-], will be used as defined in the followings.

$$Nu_{\mathrm{s}}=\frac{\alpha_{\mathrm{s}}D_{\mathrm{i}}}{\lambda_{\mathrm{s}}} \tag{6}$$

$$Re_{\mathrm{s}}=\frac{\rho_{\mathrm{s}}U_{\mathrm{m}}D_{\mathrm{i}}}{\eta_{\mathrm{s}}} \tag{7}$$

$$Pr_{\mathrm{s}}=\frac{c_{\mathrm{s}}\eta_{\mathrm{s}}}{\lambda_{\mathrm{s}}} \tag{8}$$

Here, α_s [W・m^{-2}・K^{-1}] is a heat transfer coefficient from the inner tube wall to the fluid through the inner tube; λ_s [W・m^{-2}・K^{-1}] is the thermal conductivity; ρ_s [kg・m^{-3}] is the density; η_s [Pa・s] is the viscosity; and c_s [J・kg^{-1}・K^{-1}] is the specific heat capacity of the solution without additives; Those parameters are tabulated in Table 4.

Table 4. Each physical parameter of the ammonium alum hydrate solution at 60°C.

λ_s (W·m^{-1}·K^{-1})	ρ_s (kg·m^{-3})	η_s (Pa·s)	c_s (J·kg^{-1}·K^{-1})
0.3416	1150	1.603×10^{-3}	4143

Friction coefficient, f_s [-] and Colburn's j-factor, j_s [-], defined in this paper are also calculated by the properties of the ammonium alum hydrate solution as follows.

$$f_s = \frac{\tau_{wall}}{\frac{1}{2}\rho_s U_m^2} \quad (9)$$

$$j_s = \frac{Nu_s}{Re_s Pr_s^{1/3}} \quad (10)$$

Here, τ_{wall} [Pa] is the wall shear stress on the inner tube.

2.7. Visualization of solidification in the flow

In order to visualize the solidification of the ammonium hydrate and the migration of the particles, we used a tomography method (Industrial Process Tomography, KANOMAX). A detector pipe of the tomography with the eight electrodes was connected to the test tube (Fig.3(a-c)). Electrical voltage between two electrodes was measured during constant electric current lives between the electrodes. The electrical voltage obtained in the experiments was analyzed to calculate electrical conductivity map in the cross-section of the tube. Since the electrical conductivity of ammonium alum hydrate is low, the solidification of ammonium alum hydrate in the tube was vitalized through the electrical conductivity.

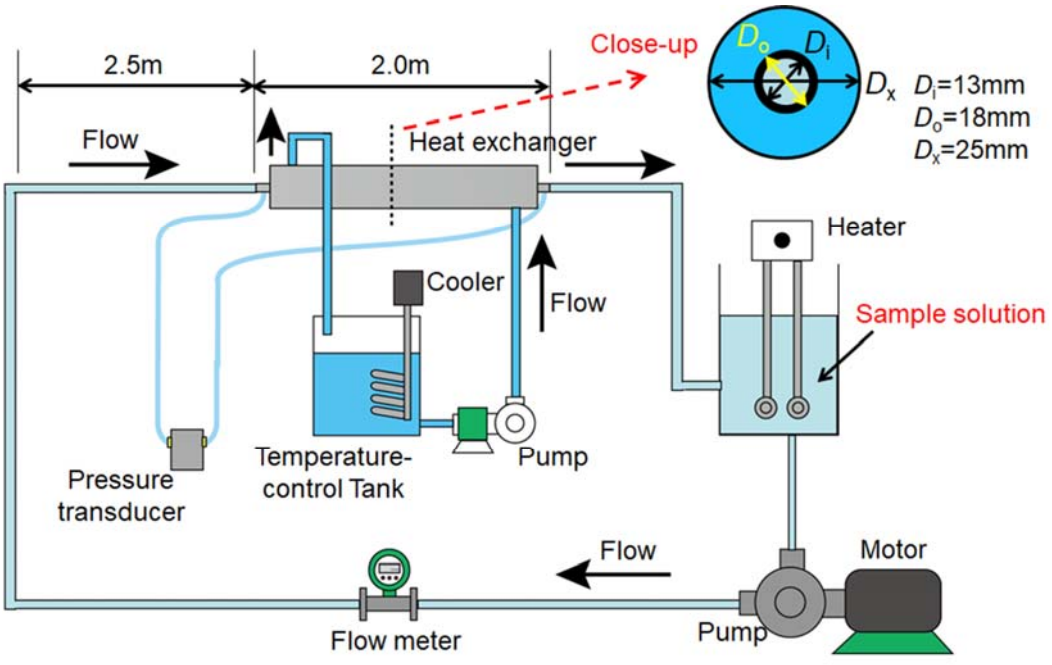

Fig.2 Schematic of the flow system to measure friction coefficients and heat transfer.

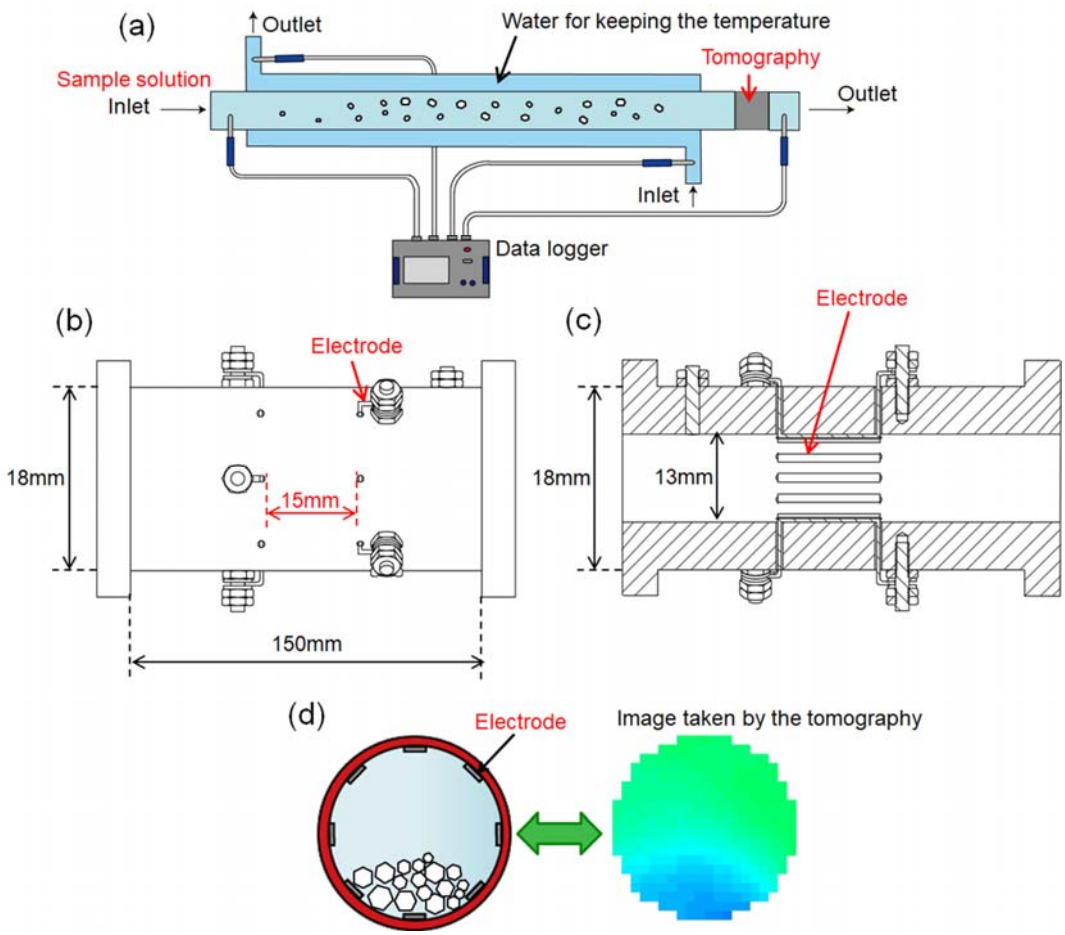

Fig.3 (a) Cross section area of the test tube. (b) A detector part of the tomography with electrodes. (c) Cross section area of the detector part. (d) Sedimentation of the particles in the tube and a tomographic image that corresponds to the sedimentation.

3. Results and Discussion

3.1. Shear Viscosity of the Hydrate Solutions and Slurries with Surfactants and PVA

Figures 4(a) and (b) show the shear viscosity of the hydrate solution and slurries, respectively. The ammonium alum hydrate solution showed Newtonian behavior and viscosity was slightly higher than that of water. When PVA was added to the solution at the concentration of 500, 1000 and 2000 ppm, the viscosities become higher. However, the solution still shows Newtonian behavior. On the other hand, when the surfactants was added to the solution at the concentration of 2000 ppm, the zero shear viscosity became much higher than the solution without the

surfactants, and the viscosity shows shear thinning behavior. The viscosity of sample solutions became higher when the PVA was also added to the solution. But the tendency of the shear thinning behavior of the surfactants added solution was not varied with the addition of PVA. This result indicated that rod-like micelles were formed in the ammonium alum hydrate solution, which was not disturbed by the addition of PVA. In the case of the ammonium alum hydrate slurries, the viscosity became higher at all the samples. Besides, the viscosity was unstable at low shear rate: This is due to fine particles of the hydrate in the slurry. But the tendency of the viscosity was the same to that of solution: The addition of PVA increased the viscosity of the hydrate slurries, and the addition of surfactants induced shear thinning behavior. Rod-like micelles were still formed in the slurries. This results proved that the drag reducing effects of the rod-like micelles remain with the addition of PVA.

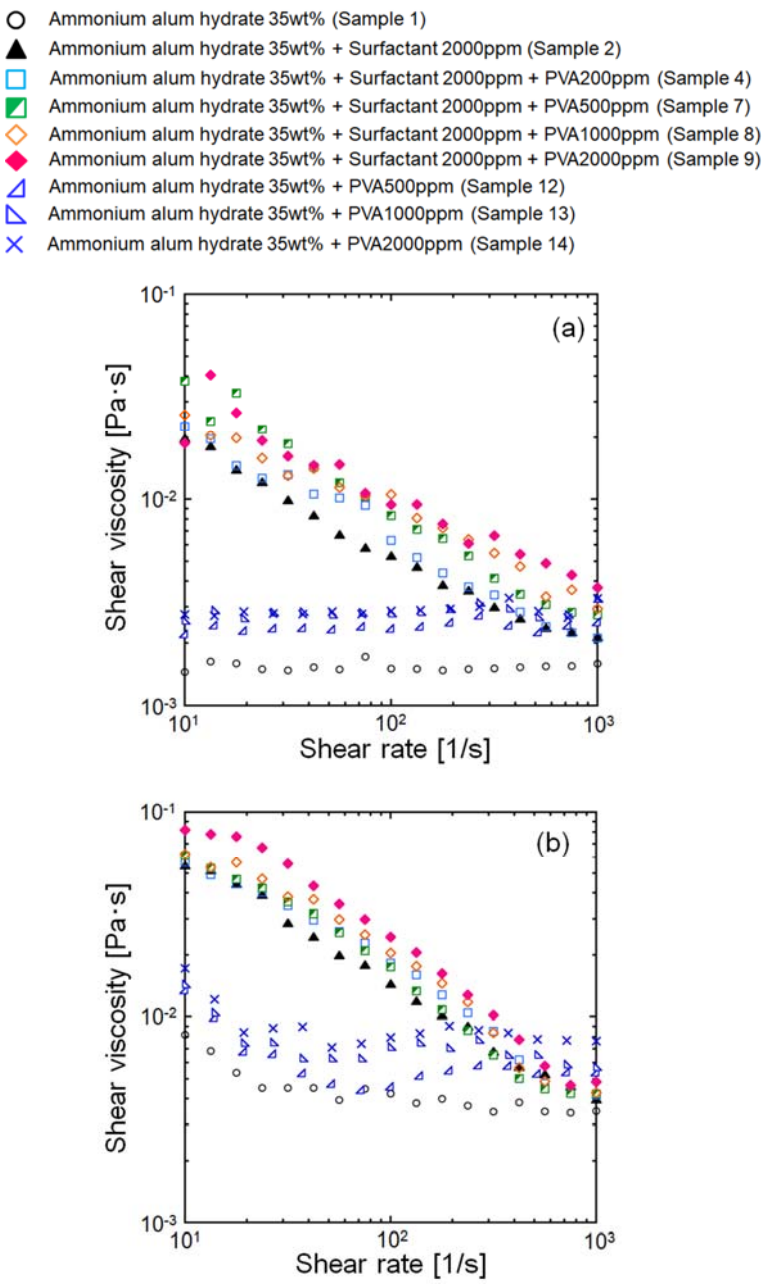

Fig.4 (a) Shear viscosity of ammonium alum hydrate solutions with additives. (b) Shear viscosity of ammonium alum hydrate slurries with additives.

3.2. Particle Sedimentation and Growth in the Hydrate Solutions with Surfactants and PVA

Figure 5 shows the sedimentation behaviors of the hydrate particles at just after sample preparation, 1 day, 3 days and 5 days after. The white hydrate particles were dispersed or settled out in the test tube. The sample numbers in the figure from 1 to 18 correspond to the samples shown in Table 1 and 2. Figure 5(a) clarifies the effects of surfactants and PVA on the sedimentation behavior; Figure 5(b) clarifies

the effects of PVA on the sedimentation behavior. When the solution didn't contain neither surfactants nor PVA, the ammonium alum hydrate particles settled out just after the sample preparation as seen in Sample 1. 2000 ppm of surfactants slightly delayed the sedimentation, but it occurred by no later than 1 day as seen in Sample 2. When sample solutions contain both surfactants and PVA, the sedimentation was clearly delayed (Samples 3 – 9). Interestingly, the effect of PVA appeared only when the surfactants were also added to the solution. The particles settled out in one day completely in the solution containing only PVA at the concentration of 14000 ppm that is two times of the overlap concentration of PVA (Samples 10 – 18). In order to quantify the sedimentation behavior, an apparent dispersion fraction that is explained in the experimental section and Fig. 1(b) was calculated: The results are shown in Fig. 6. The sedimentation behavior of Samples 1 and 12 – 14 were almost the same. The particles were settled out just after the sample preparation. When the solution contains both surfactants and PVA, the sedimentation delayed for several days. An effect was started to be observed when 200 ppm of PVA added to the 2000 ppm surfactant solution (Sample 4). The effect became more efficient with 500 ppm PVA additives. When the concentration of PVA reached 1000 ppm, the hydrate particles didn't settle out for about 4 days.

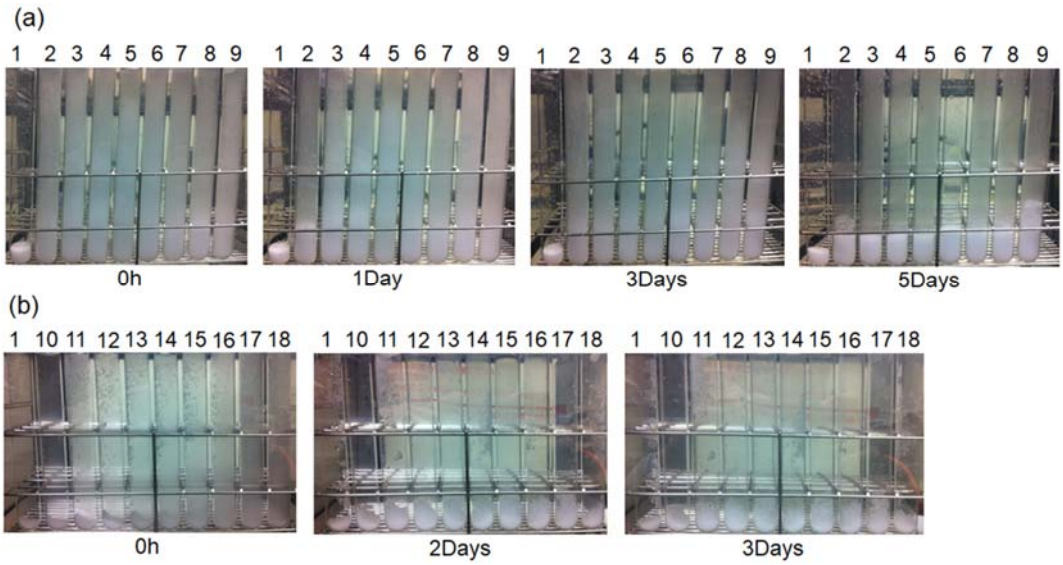

Fig.5 Sedimentation of the ammonium alum particles in the solutions. (a) Ammonium alum hydrate solutions with surfactants and PVA. (b) Ammonium alum hydrate solutions with PVA.

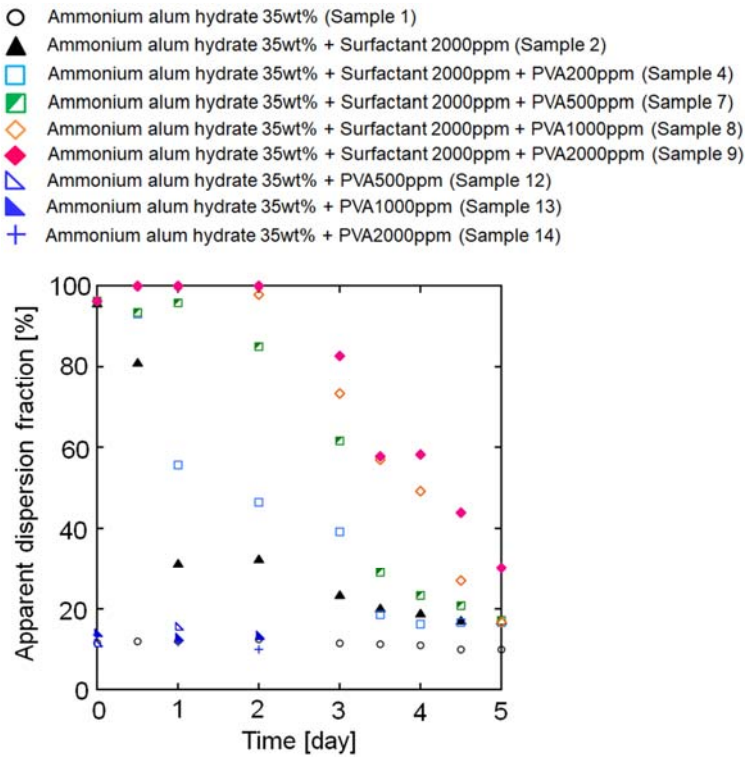

Fig.6 Apparent dispersion fraction of annmonium alum hydrate particles in each sample solution.

If the sedimentation behavior was just affected by the solution viscosity, the hydrate particles could have been sunk in about 13 hours even in Sample 9 that contain both 2000 ppm of surfactants and PVA. The sedimentation time is assumed by the initial length as shown in Figure 1(b) divided by a mean velocity. The mean velocity was calculated by Stokes equation.

$$6\pi r\eta v = \frac{4\pi r^3}{3}(\rho_h - \rho_s)g \qquad (11)$$

Here, r [m] is mean radius of particle just after the sample preparation obtained from the median diameter; η [Pa□s] is the zero shear viscosity of each solution; v [m□s^{-1}] is the mean velocity; ρ_h [kg□m-^{3}] is the density of the ammonium alum hydrate, ρ_s [kg□m^{-3}] is the density of the hydrate solution at 60°C, and g [m□s^{-2}] is the gravitational acceleration. The sedimentation time of Sample 9 containing both 2000 ppm of surfactants and PVA is the longest. However, 13 hours is much shorter than the observed sedimentation time as shown in Fig. 6. Therefore, not only the viscosity but also other reasons exist to prohibit sedimentation.

Particle growths in each solution was also recorded for 6 hours as shown in Fig. 7. These images were taken at different positions to confirm the characteristics of the particle growths in each case. Ammonium alum hydrates particles in the solution containing neither surfactants nor PVA grew uniformly as shown in Sample 1. The particle growths in the solution containing surfactants became slightly non-uniform: Small and large particles were seen at 2 hours later. However, the particles became uniformly large at 6 hours later. In the case of Sample 9 containing both surfactants and PVA at 200ppm, the particle growth was not uniform: Many small particles were observed at 6 hours later. In the case of Sample 14 containing only PVA, particles became much larger than that in Sample 9. Figure 8 shows cumulative percentage of the particle sizes of each image at the beginning of the experiments and 6 hours later. Particle sizes were shifted to larger size in 6 hours. When both surfactants and PVA were added to a solution, particle growths were prohibited. Figure 9 shows median diameters of each cumulative percentage, which represent the mean particle size. The median diameter of the particles in Sample 1 was increased linearly for 6 hours. The median diameter was increased non-linearly in solutions containing both surfactants and PVA, especially in Samples 8 and 9. The particle growth was slightly prohibited in Samples 13 and 14 that contain only PVA. These data also indicate a combined effect of surfactants and PVA.

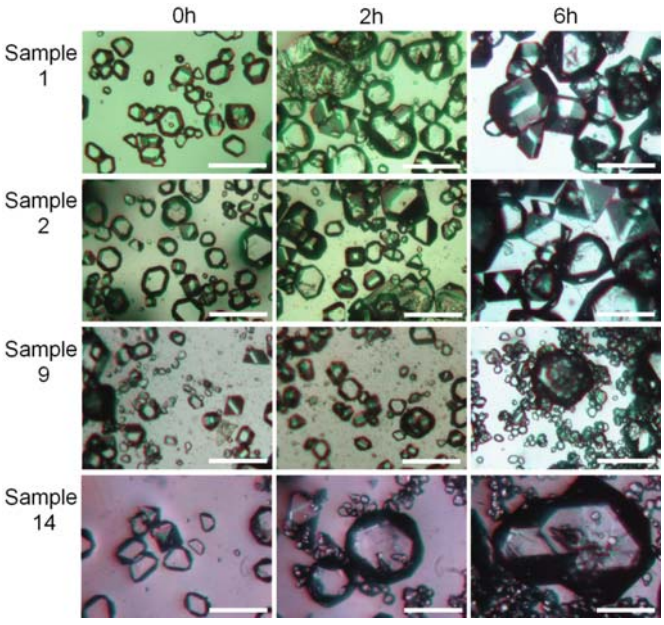

Fig.7 Particle growth in each sample solution within 6 hours observed by a microscope

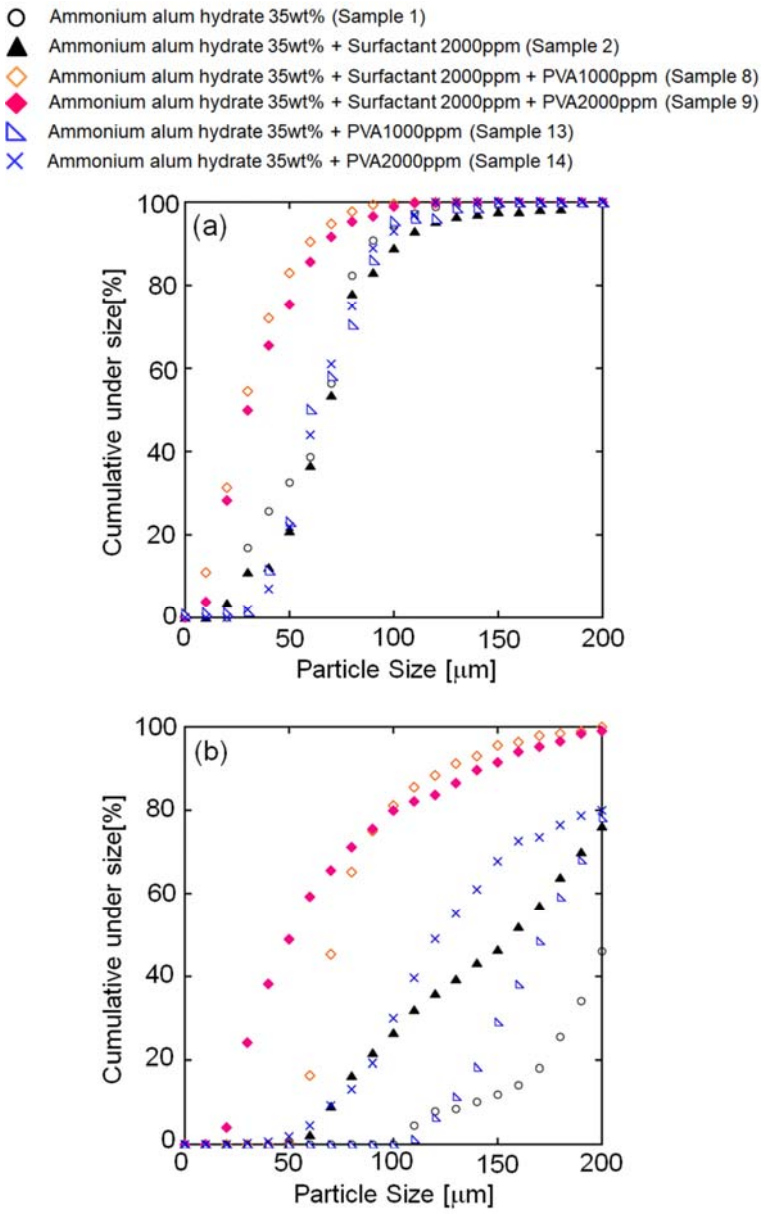

Fig.8 Cumulative under size of particles in each sample solution. (a) Distributions measured just after observation. (b) Distributions measured at 6 hours from the beginning of the experiments.

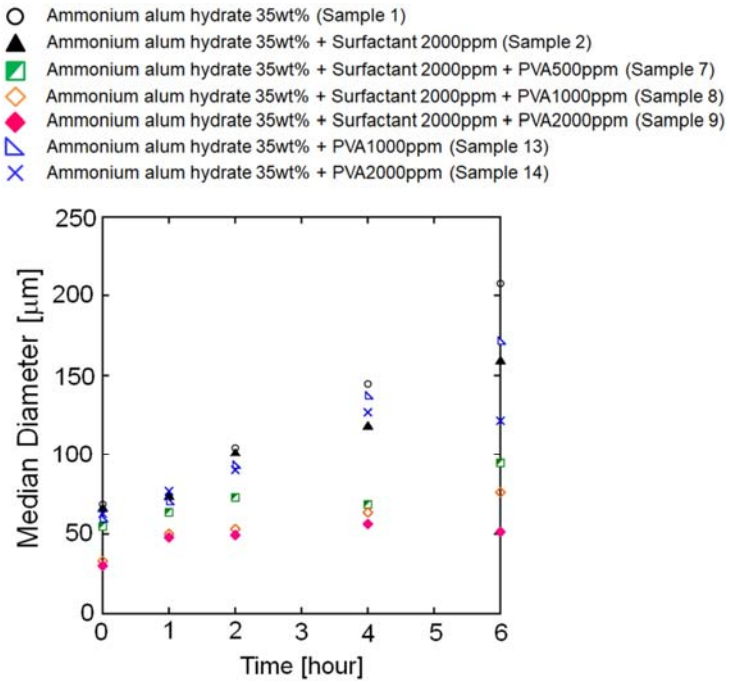

Fig.9 Median diameter of the particle size in each sample solution.

The results of the sedimentation experiment and the particle growth experiment indicate there is a combined effect of surfactants and PVA. Polymer chains in a solution are attached to each other over the overlap concentration. Therefore, it is natural to doubt network structure of PVA to prevent the sedimentation and the particle growth. However, the overlap concentration of PVA in this study is 7000 ppm indeed. Thus, PVA at the concentration of 2000 ppm that efficiently works with surfactants is too low for the overlap concentration. In addition, when the solution contains only PVA, PVA didn't work efficiently at 14000 ppm that is twice of the overlap concentration.

In order to detect a combined effect of PVA and surfactants, an inner structure of sample solutions was measured by DLS. Hydrodynamic diameter measured by the DLS is shown in Fig. 10(a). To validate the present experimental data, the diameter of coiled PVA was measured at concentrations of 1,000 and 2,000 ppm solutions. In this case, surfactants were not added. The diameter of PVA was 9.26 nm in the 1000 ppm solution and 14.1 nm in the 2000 ppm solution. The theoretical diameter (Flory diameter) of the structure is 12.74 nm; therefore, the experimental results are in reasonable agreement. In Fig. 10(a), we can see two characteristic lengths, L_1 and L_2, in almost all the sample solutions. L_1 was ~10 nm and L_2 was ~80 nm. When the solution contains only surfactants and counter-ions (Sample A), only the two characteristic lengths L_1 and L_2 were measured. In the

solution, surfactants form rod-like micelles, therefore L_1 and L_2 were due to the rod-like micelles. L_1 corresponds to a diameter of the rod-like micelles; L_2 corresponds to the length of the micelles (Fig. 10(b)). The characteristic length was not varied when the concentration of PVA was low as 200 ppm (Sample B). When the concentration of PVA is higher than 500 ppm (Sample C), a longer characteristic scale (L_3) that is approximately 120 to 145 nm appears. The cationic surfactant used in this study has an electropositive hydrophilic head. However, in the present study, the surfactant is non-ionized with counter-ions. The interaction between PVA and ionic and nonionic surfactants was a long-standing issue. In general, surfactants are likely to attach PVA. Therefore, we can consider PVA was surrounded by surfactant micelles. While it is difficult to describe how the surfactants attach to PVA, we assumed aggregated structure that is shown in Figs 10(c) and (d). PVA can be stretched by the effect of surrounding surfactant micelles, as the core of a rod-like structure shown in Figs 10(b) and (c). When PVA, of which the polymerization degree is 500, is stretched, the length would be approximately 150 nm. The length is calculated simply from the diameter of the monomer, 0.3 nm, and the polymerization degree, 500, as 0.3×500 nm^2. The length 150 nm is close to L_3, therefore, our assumption is reasonable: The length L_3 is the stretched PVA surrounded by surfactants. When the concentration of PVA is even higher, 1000 and 2000 ppm (Sample D, E), a further larger scale (L_4) appeared. L_4 is considered due to an aggregated structure of PVA and surfactants as shown in Fig. 10(d).

We considered how these structures function to prevent the sedimentation of ammonium alum hydrates. As described above, viscosity increase and overlap concentration cannot explain the phenomena. We focused on how much volume can be occupied by such inner structures. In the case of Sample A, surfactants form rod-like micelles. When the rod-like micelles are considered as tubes, the volume of each rod-like micelle V_m [m^3], is calculated by L_1 [m] and L_2 [m]:

$$V_m = \frac{\pi L_1^2}{4} \times L_2 \qquad (12)$$

Then, we calculated how many tube structure as shown in Figs 10(b) to (d) were possible to form in each sample solution by taking into account the number of surfactant molecules. The number of surfactant molecules N_{sur} [-] that form a rod-

like micelle was assumed from L_1 [m], L_2 [m] and the diameter of the head of the surfactant, l_{head} [m]: where l_{head} [m] is estimated to be approximately 0.3 nm:

$$N_{sur} = \frac{\pi L_1}{l_{head}} \times \frac{L_2}{l_{head}} \quad (13)$$

The number of the rod-like micelles N_{rod} [-] was calculated from N_{rod} [-] = N_{total} [-] / N_{sur} [-]: N_{total} [-] is the total number of surfactant molecules in the solution, which was calculated from the concentration of the surfactant solution. Finally, the total volume of the rod-like micelles $V_{micelle}$ [m^3], in Sample A was estimated:

$$V_{micelle} = N_{rod} \times V_m \quad (14)$$

The total volume of a tube structure that is the combined structure of the surfactants and PVA were also calculated in the same way as $V_{micelle}$ [m^3]. In the case of Sample B, although PVA was added to the solution only L_1 [m] and L_2 [m] were measured: PVA was considered to be inside the rod-like micelles. To calculate the total volume of the tube structure, the number of the surfactant-PVA tube structure was considered to be the number of PVA molecules in the Sample B solution. This is because; less number of surfactant molecules can make a rod-like micelles in the presence of PVA. In the case of Samples C to E, tube structures defined by the diameter of the cross-section L_1 [m] and lengths L_2 [m], L_3 [m] and L_4 [m] were formed in the solution. The number of tube structures was considered to be the number of PVA molecules in the solution. In the case where several lengths of structures were observed in the same solution, such as Samples D and E, the number of structures was simply obtained from the number of PVA molecules divided by the number of structures. When the number of tube structures in each solution was obtained, the total occupation volume of the tube structures $V_{structure}$ [m^3], in the solution was calculated in the same way as rod-like micelles shown in Eq. (14).

The percentage of occupation of the rod-like micelles and tube structures γ [%] to the solution volume V_{sol} [m^3] was calculated by

$$\gamma = \frac{V_{\text{micelle}}}{V_{\text{sol}}} \times 100\,, \quad \gamma = \frac{V_{\text{structure}}}{V_{\text{sol}}} \times 100 \qquad (15)$$

The percentage of occupation in volume γ [%] is shown in Fig. 11. γ [%] of Sample A was almost 0%. The value of γ [%] was increased when PVA was added to the solution. γ [%] reached more than 50% at PVA 500 ppm; γ [%] reached more than 100% at PVA 2000 ppm: It was possible the volume of solution was totally occupied by tube structures. The effect of PVA on the variation of γ [%] is dramatic. Thus, it is possible that the occupation by the tube structures in solution can prevent the sedimentation of ammonium alum hydrate. This proposal reasonably explained the results of Fig. 6.

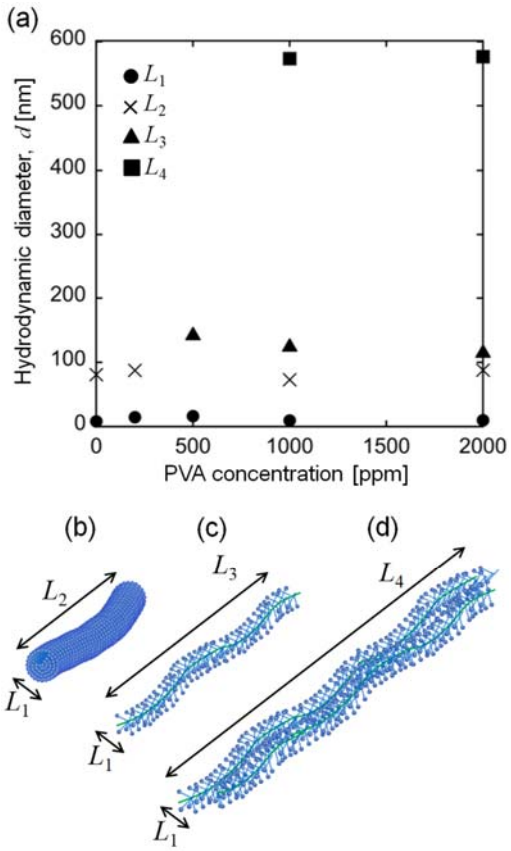

Fig. 10. (a) Hydrodynamic diameter observed in each solution as a function of the PVA concentration. (b) Schematic illustrations of rod-like micelles, (c) the combined structure with PVA at low PVA concentrations and (d) at high PVA concentrations.

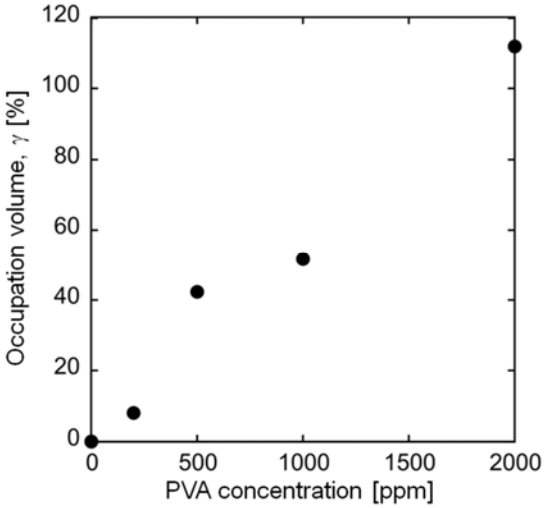

Fig. 11. Occupation volume of structures to the solution volume, γ [%].

Figure 12 shows frictional coefficients of the hydrate solutions and slurries. Reynolds numbers, *Re*, were calculated by using the viscosity of ammonium alum hydrate solution without additives. In the figure, theoretical values for the laminar flow of Newtonian fluid, $f_s = 16/Re_s$, is shown by the solid line; the empirical equation of Blasius' frictional coefficient, $f_s = 0.0791 Re_s^{-0.25}$, for the turbulent flow of Newtonian fluid is also plotted by solid lines. The viscosity of the sample solutions that contain surfactants or PVA were slightly higher than that of the ammonium alum hydrate solution without additives, therefore, *Re* of the sample solution with additives was slightly shifted to higher value compared with $f_s = 16/Re_s$ or $f_s = 0.0791 Re_s^{-0.25}$ (Fig.12(a)). Frictional coefficients of the hydrate slurries are also plotted to *Re* calculated by the viscosity of solution. Thus, the gap in the abscissa axis is slightly larger than that of solutions (Fig.12(b)). As seen in the results of Sample 2, surfactants added to the hydrate solutions and slurries decrease the friction coefficients due to the formation of the drag-reducing rod-like micelles. In addition, the importance of this figure is that PVA did not affect the friction coefficient of the solutions (Sample 8) and slurries (Sample 13); that is, the formation of rod-like micelles was not disturbed by PVA.

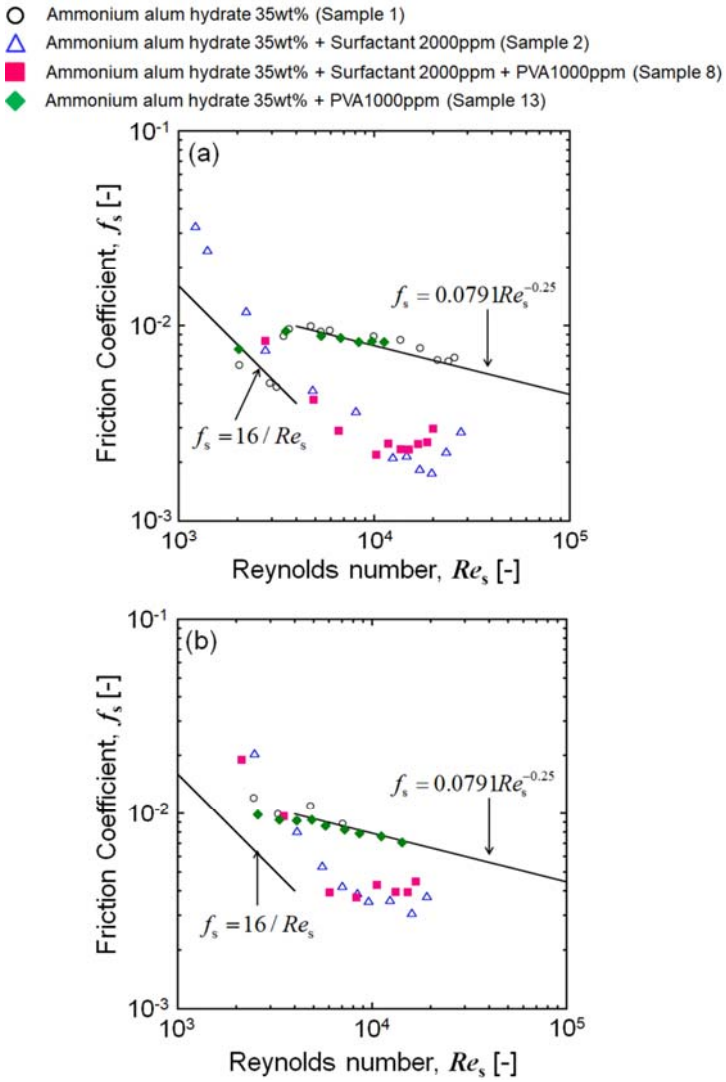

Fig. 12. Friction coefficient of ammonium alum hydrate solutions (a) and slurries (b).

Figure 13 shows Nusselt numbers, *Nu*, of the hydrate solutions and slurries. *Nu* of water is also plotted in Fig.13 (a) for a comparison. The dotted line in Fig.13 (a) shows Dittus-Boelter's equation calculated by Eq. (1). As shown in the figure, the heat transfer coefficients of water follow Eq. (1) very well: That was also reported in our previous studies [30, 31]. Thus, the Dittus-Boelter's equation is reasonable to evaluate experiments in this study. In Fig. 13, *Re* of the hydrate solutions and slurries was calculated by using the viscosity of ammonium alum solution without additives. The solid line in the figure shows Dittus-Boelter's equation calculated with ammonium alum hydrate solution properties. The experimental data of the hydrate solution (Sample 1) shown in Fig. 13(a) fit well to Dittus-Boelter's equation. As seen in the results of Sample 2 and Sample 8,

surfactants added to solutions decrease the heat transfer characteristics, *Nu*. When PVA was added to solutions (Sample 13), *Nu* was almost the same to that of the hydrate solution (Sample 1).

In the case of the hydrate slurry, heat transfer was higher than that of the solution. This is because temperature differences became smaller due to phase transition in the flow. Therefore, apparent heat capacity became larger: *Nu* increases. Zhang et al [22] tried to explain this phenomenon by considering Stephan number, but it cannot apply to our data since the effect of Stephan number on Nusselt number has not been clarified. Here, supercooling did not occur during the solidification process: Pump pressure helped to prohibit supercooling. In addition, we have confirmed the solidication process at the phase change temperature by using the tomography method. When surfactants were added to slurries, *Nu* was decreased same as the solution. This is due to laminarization of rod-like micelles. Besides, in the hydrate slurry case, Sample 8 that contain both surfactants and PVA showed lower *Nu* compared with that of the solution. The decrease of *Nu* with PVA additives seemed unpleasant results in terms of preventing the sedimentation. Therefore, we calculated Colburn's j-factor in order to see the heat transfer efficiency.

Figure 14 shows the Colburn's *j*-factor, j_s [-], divided by the friction coefficient, f_s [-]. In the figure, the solid lines show the j_s/f_s calculated with Dittus-Boelter's equation and Blasius' equation. In the case of solution, j_s/f_s was increased when the solution contains surfactants. On the other hand, j_s/f_s of the hydrate solution and PVA added solution was decreased. In the case of slurry, all j_s/f_s values were higher than that of solution. Therefore, the results of j_s/f_s confirm the efficiency of heat transfer to fluids transportation.

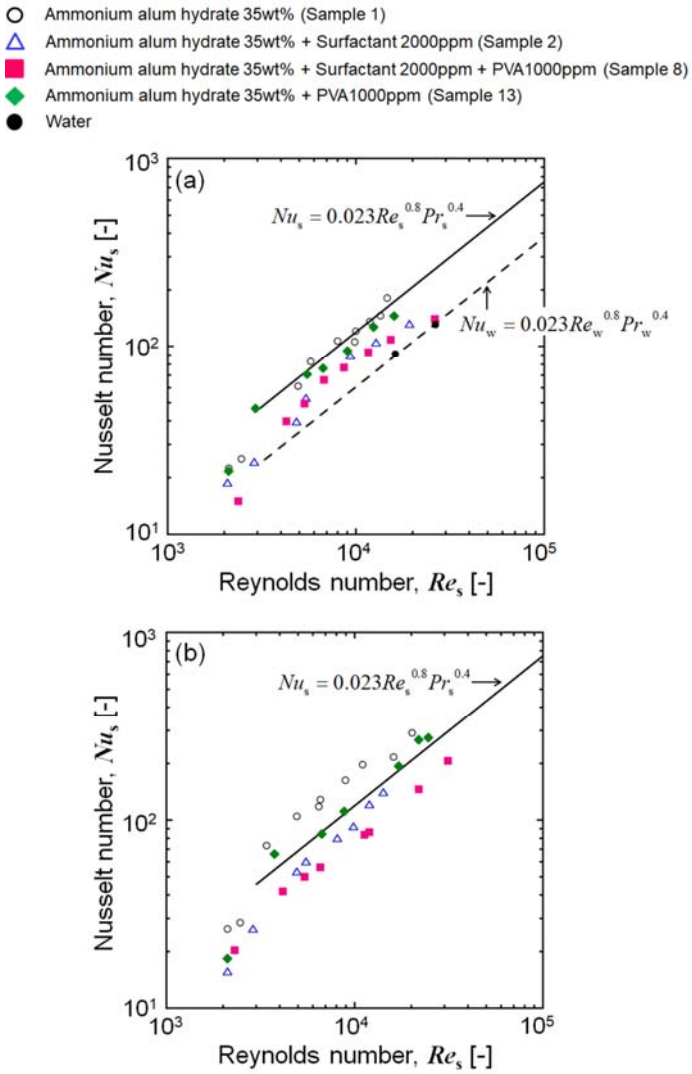

Fig. 13. Nusselt number of water and ammonium alum hydrate solutions (a) and slurries (b).

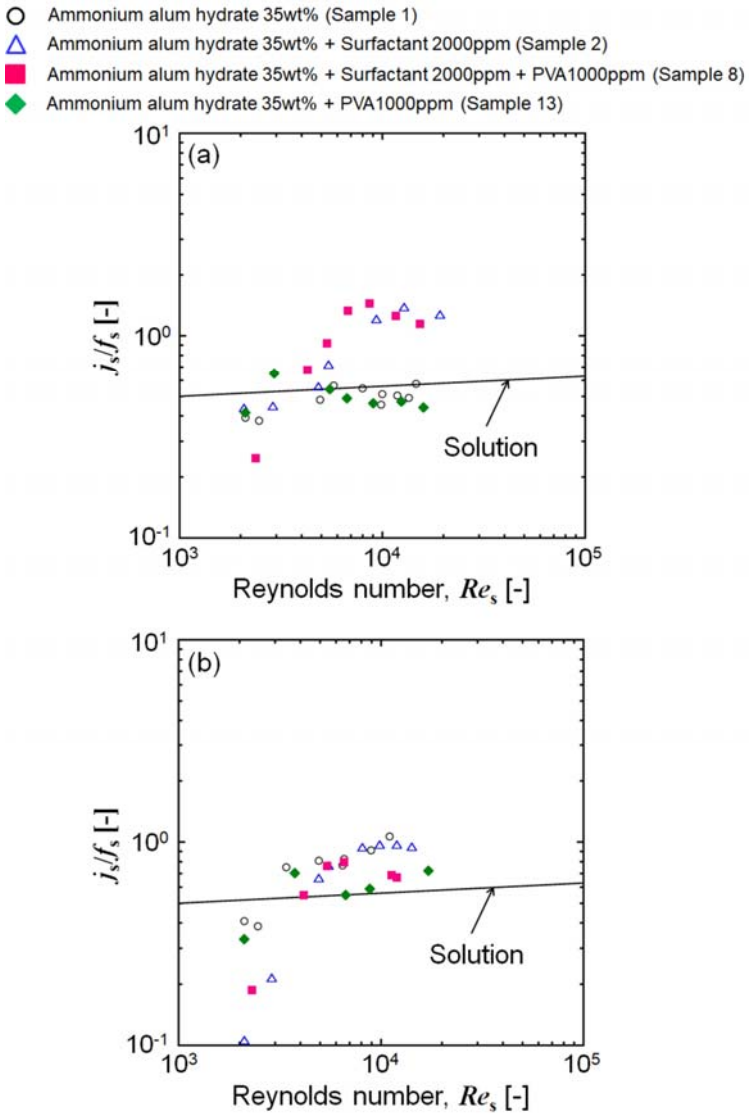

Fig. 14. Colburn's j-factor, j_s [-], divided by the friction coefficient, f_s [-]. (a) j_s/f_s of alum hydrate solutions and (b) slurries.

Results of electrical conductivity of each solution in the tube at several flow rates and at each temperature are shown in Fig. 15. The electrical conductivity visualizes the solidification of ammonium alum hydrate. The electrical conductivity of all sample solutions is relatively high at the initial temperature of the heat transfer experiment about 54 °C: the result indicates ammonium alum was dissolved in each sample solution. The value of the electrical conductivity of all sample solutions was decreased at the phase change temperature about 51°C: the solidification of ammonium alum starts. Then the value was further decreased at 50°C that is the temperature at the exit of the test tube. In the case of Sample 1 and Sample 13, the electrical conductivity was especially low at the bottom of the tube at Re_s=2100 (Figs 15(a) and (d)): the result indicates the sedimentation of the ammonium alum

solid particles. On the other hand, it seems that the sedimentation was prohibited in Sample 8 (Fig. 15(c)). It is again confirmed that the addition of surfactants and PVA to the solution prohibits the sedimentation of the ammonium alum particles in the flow. It is promising results for industrial application of ammonium alum hydrate slurries.

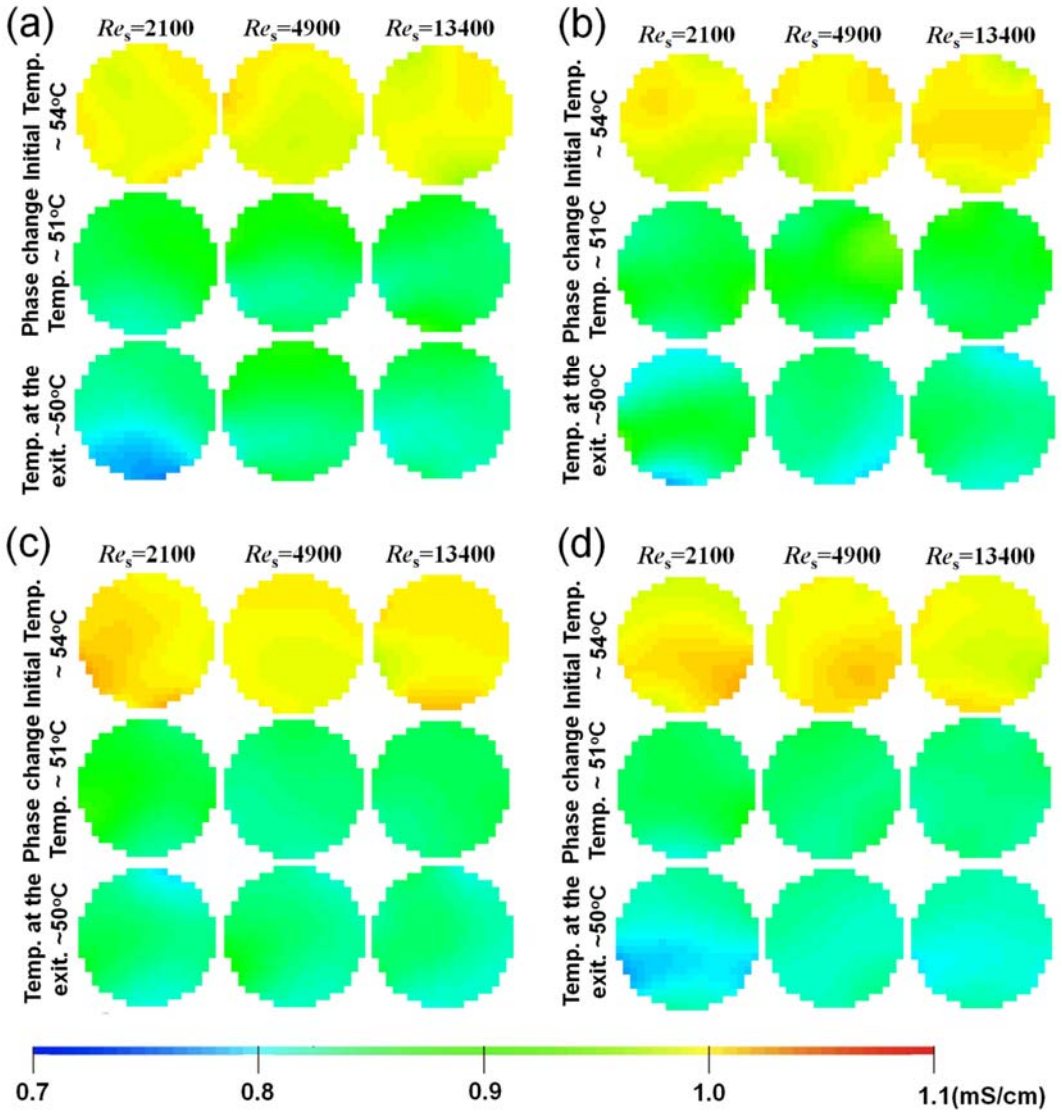

Fig. 15. Electrical conductivity in the test tube. (a) Ammonium alum hydrate solution, Sample 1. (b) Ammonium alum hydrate + surfactant 2000 ppm solution, Sample 2. (c) Ammonium alum hydrate + surfactant 2000 ppm + PVA 1000 ppm solution, Sample 8. (d) Ammonium alum hydrate + PVA 1000 ppm solution, Sample 13.

4. Conclusion

We aimed to develop recently proposed latent heat transportation materials for higher temperature for industrial application. The latent heat material is ammonium alum hydrate that was firstly proposed in our previous studies: The phase change temperature is able to be controlled by its concentration. High phase change temperature at 51°C is achieved at 35wt% of the ammonium alum hydrate. The temperature around 50°C is promising for waste heat utilization from industrial plants. However, the density of the ammonium alum hydrate is higher than water. Therefore, a technique was required to prevent sedimentation of the ammonium alum hydrate particles in the latent heat transportation slurries. The sedimentation of the particles causes pipe blockage in the system, which is a severe problem.

In this study, we add drag reducing surfactants and polyvinyl alcohol (PVA) in solution of ammonium alum hydrate to increase fluidity and to prevent sedimentation. The effects of surfactants and PVA was precisely analyzed in terms of crystal growth of the ammonium alum hydrate particles, sedimentation, fluidity, heat transfer characteristics. Main concluding remarks obtained in the present study are follows.

1. Addition of PVA did not affect flow properties. Viscosity of ammonium alum hydrate solution and slurries with and without PVA were almost the same. The viscosity of ammonium alum hydrate with surfactants solution and slurries were also not affected by PVA: The results indicated PVA did not disturb the formation of rod-like micelles of the surfactant.

2. Sedimentation and crystal growth of ammonium alum hydrate were significantly delayed when the solution contains both surfactant at 2000 ppm and PVA at certain concentration. When the concentration of PVA was 500 ppm, the effect of PVA became obvious. When the concentration of PVA was 1000 ppm, the ammonium alum hydrate particles were dispersed for more than 4 days: The term is enough long for practical use. On the other hand, when PVA was solely added to the ammonium alum hydrate solution, the sedimentation and crystal growth were not prohibited.

3. The delay of the sedimentation was not explained by increase of the viscosity of the solution. Therefore, solutions contain surfactants and PVA without ammonium alum hydrate at several concentrations were measured by DLS in order to detect combined effects. From the results, it seemed rod-like micelles became longer with

the addition of PVA. Therefore, combined structure made of rod-like micelles and PVA can occupy the solution: the structure can delay the sedimentation of the ammonium alum particles.

4. Fluidity of the ammonium alum hydrate solution and slurry with or without surfactants was not affected by PVA. However, heat transfer characteristics were decreased with the addition of surfactants and PVA: this is due to the drag reducing effects and increase of viscosity. However, Colburn's *j*-factor, j_s, divided by the friction coefficient, f_s, that is j_s/f_s, of all the ammonium alum hydrate slurries with surfactants and PVA were higher than ammonium alum hydrate solution. Therefore, the efficiency of the heart transportation was increased.

5. Sedimentation of the ammonium alum hydrate in a flow was visualized by a tomography method. Surfactants and PVA effectively prohibited the sedimentation of the particles.

From the results, we solved main problems of ammonium alum hydrate slurries, that is, low fluidity and sedimentation for industrial application. We are now going to make a feasibility study in a real plant.

Reference

[1] M. Tamaru, H. Suzuki, R. Hidema, Y. Komoda, K. Suzuki, Fabrication of hard-shell microcapsules containing inorganic materials, Int. J. Refrig. 82 (2017) 97-105

[2] P. Zhang, Z.W. Ma, Z.Y. Bai, J. Ye, Rheological and energy transport characteristics of a phase change material slurry, Energy. 106 (2016) 63-72

[3] J. Oignet, A. Delahaye, J.-P. Torréb, C. Dicharry, H.M. Hoang, P. Clain, V. Osswald, Z. Youssef, L. Fournaison, Rheological study of CO_2 hydrate slurry in the presence of Sodium Dodecyl Sulfate in a secondary refrigeration loop, Chem. Eng. Sci. 158 (2017) 294-303.

[4] J. Oignet, H.M. Hoang, V. Osswald, A. Delahaye, L. Fournaison, P. Haberschill, Experimental study of convective heat transfer coefficients of CO_2 hydrate slurries in a secondary refrigeration loop, Appl. Thermal Eng. 118 (2017) 630-637.

[5] H. Kumano, Y. Yamanada, Y. Makino, T. Asaoka, Effect of initial aqueous solution concentration on rheological behavior of ice slurry, Int. J. Refrig. 68 (2016) 218-225.

[6] J. Bellas, I. Chaer, S.A. Tassou, Heat transfer and pressure drop of ice slurries in plate heat exchangers, Applied Thermal Eng. 22 (7) (2001) 721-732.

[7] H. Inaba, T. Inada, A. Horibe, H. Suzuki, U. Usui, Preventing Agglomeration and Growth of Ice Particles in Water with Suitable Additives, Int. J. Refrig. 28 (2005) 20-26.

[8] D. W. Lee E. S. Yoon, M. C. Joo, A. Sharma, Heat transfer characteristics of the ice slurry at melting process in a tube flow, Int. J. Refrig. 29 (2006) 451-455.

[9] J. Wang, S. Wang, T. Zhang, F. Battaglia, Mathematical and experimental investigation on pressure drop of heterogeneous ice slurry flow in horizontal pipes, Int. J. Heat. Mass. Trans. 108 (2017) 2381-2392.

[10] S. Grandum, A. Yabe, M. Tanaka, F. Takemura, K. Nakagomi, Characteristics of ice slurry containing antifreeze protein for ice storage applications, J. Thermophys. Heat Trans. 11 (1997) 461-466.

[11] S. Grandum, A. Yabe, K. Nakagomi, M. Tanaka, F. Takemura, Y. Kobayashi, P.E. Frivik, Analysis of ice crystal growth for a crystal surface containing adsorbed antifreeze proteins, J. Cryst. Growth, 205 (1999) 382–390.

[12] T. Inada, A. Yabe, S. Grandum, T. Saito, Control of molecularlevel ice crystallization using antifreeze protein and silane coupling agent, Mater. Sci. Eng. A, 292 (2000) 149-154.

[13] T. Inada, A. Yabe, S. Grandum, T. Saito, Ice storage system with water–oil mixture formation of suspension with high IPF, Int. J. Refrig. 23 (2000) 336-344.

[14] K. Matsumoto, Y. Shiokawa, M. Okada, T. Kawagoe, C. Kang, Ice storage system using water–oil mixture. Discussion about influence of additive on ice formation process, Int. J. Refrig. 25 (2002) 11-18.

[15] H. Suzuki, K. Nakayama, Y. Komoda, H. Usui, K. Okada, R. Fujisawa, Particle Size Characteristics of Ice Slurry Treated with Surfactants and Brines, J. Chem. Eng. Japan, 42 (6) (2009) 447-451.

[16] H. Suzuki, T. Konaka, Y. Komoda, Particle Size Depression and Drag Reduction of Ice Slurry Treated with Combination Additives of Surfactants and Poly(vinyl alcohol), J. Chem. Eng. Japan. 43 (2010) 482-486.

[17] S.S. Lu, T. Inada, A. Yabe, X. Zhang, S. Grandum, Microscale Study of Poly(vinyl alcohol) as an Effective Additive for Inhibiting Recrystal-lization in Ice Slurries, Int. J. Refrig. 25 (2002) 563–569.

[18] M. Darbouret, M. Cournil, J. M. Herri, Reological Study of TBAB Hydrate Slurries as Secondary Two-Phase Refrigerants, Int. J. Refrig. 28 (2005) 663-671.

[19] Y. S. Indartono, H. Usui, H. Suzuki, Y. Komoda, K. Nakayama, Hydrodynamics and Heat Transfer Characteristics of Drag-Reducing Trimethyloethane Solurion and Suspension by Cationic Surfactant, J. Chem. Eng. Japan. 39 (2006) 623-632.

[20] H. Suzuki, N. Wada, H. Usui, Y. Komoda,, S. Ujiie, Drag-Reduction of Trimethylolethane Hydrate Slurries Treated with Surfactants, Int. J. Refrig. 32 (2009) 931-937.

[21] Z. W. Ma, P. Zhang, R. Z. Wang, S. Furui, G. N. Xi, Forced flow and convective melting heat transfer of clathrate hydrate slurry in tubes, Int. J. Heat. Mass. Trans. 53 (2010) 3745-3757.

[22] P. Zhang, J. Ye, Experimental investigation of forced flow and heat transfer characteristics of phase change material slurries in mini-tubes, Int. J. Heat. Mass. Trans. 79 (2014) 1002-1013.

[23] H. Kumano, T. Hirata, T. Kudoh, Experimental study on the flow and heat transfer characteristics of a tetra-n-butyl ammonium bromide hydrate slurry (second report: Heat transfer characteristics), Int. J. Refrig. 34 (2011) 1963-1971.

[24] Zakin, J.L., Lu, B., Bewersdorf, H-W., “Surfactant drag reduction,” Rev. Chem. Eng., 14, pp. 253–320 (1998).

[25] H. Suzuki, H. Higuchi, H. Watanabe, Y. Komoda, S. Ozawa, T. Nishimura, N. Takenaka, Relaxation Behavior of a Drag-Reducing Cationic Surfactant Solution, Nihon Reoroji Gakkaishi. 40 (2012) 85-90.
[26] J. Rozanski, Heat transfer in the thermal entrance region for drag reduction surfactant solutions in pipe flow, Int. J. Heat. Mass. Trans. 55 (2012) 1113-1125.
[27] H. Usui, T. Kamada, H. Suzuki, Surfactant Drag Reduction Caused by a Cationic Surfactant with Excess Addition of Counter-ions, J. Chem. Eng. Japan. 37 (2004) 1232-1237.
[28] H. Suzuki, G.G. Fuller, T. Nakayama, H. Usui, Development Characteristics of Drag-Reducing Surfactant Solution Flow in a Duct, Rheol. Acta. 43 (2004) 232-239.
[29] H. Suzuki, H.P. Nguyen, T. Nakayama, H. Usui, Development Characteristics of Fluctuating Velocity Field of Drag-Reducing Surfactant Solution Flow in a Duct, Rheol. Acta. 44 (2005) 457-464.
[30] H. Suzuki, T. Kishimoto, Y. Komoda, H. Usui, Investigation of Thermal Properties of Na_2HPO_4 Hydrate Slurries for Evaluating Their Use as a Coolant in Absorption Chillers, J. Chem. Eng. Japan. 43 (2010) 34-39.
[31] H. Suzuki, T. Konaka, Y. Komoda, T. Ishigami, Flow and heat transfer characteristics of ammonium alum hydrate slurries, Int. J. Refrig. 36 (2013) 81-87.
[32] R. Hidema, T. Tano, H. Suzuki, M. Fujii, Y. Komoda, T. Toyoda, Phase separation characteristics of ammonium alum hydrates with poly vinyl alcohol, J. Chem. Eng. Japan. 47 (2014) 169-174.
[33] R. Hidema, T. Toyoda, H. Suzuki, Y. Komoda, Y. Shibata, Adhesive behavior of a calcium carbonate particle to solid walls having different hydrophilic characteristics, Int. J. Heat. Mass. Trans. 92 (2016) 603-609.